Journal of the Taiwan Institute of Chemical Engineers 63 (2016) 506–511

Contents lists available at ScienceDirect

Journal of the Taiwan Institute of Chemical Engineers

journal homepage: www.elsevier.com/locate/jtice

Novel synthesis of Ag_3PO_4/CNFs/silica-fiber hybrid composite as an efficient photocatalyst

Pengfei Chen, Li Zhang, Qiang Wu*, Weifeng Yao

Shanghai Key Laboratory of Materials Protection and Advanced Materials in Electric Power, College of Environmental and Chemical Engineering, Shanghai University of Electric Power, Shanghai 200090, China

ARTICLE INFO

Article history:
Received 8 December 2015
Revised 29 February 2016
Accepted 15 March 2016
Available online 2 April 2016

Keywords:
Carbon nanofibers (CNFs)
Chemical vapor deposition (CVD)
Hydrothermal
Silver orthophosphate (Ag_3PO_4)
Visible-light photocatalysis

ABSTRACT

Novel Ag_3PO_4/CNFs/silica-fiber composite photocatalyst was successfully synthesized via a facile combined chemical vapor deposition (CVD) technique and hydrothermal process. The as-prepared Ag_3PO_4/CNFs/silica-fiber was characterized by X-Ray diffraction, field emission scanning electron microscopy, ultraviolet–visible diffuse reflectance spectroscopy, and photoluminescence spectroscopy. The photocatalytic activity of Ag_3PO_4/CNFs/silica-fiber was evaluated by the degradation of rhodamine B (RhB) under visible-light irradiation. Note that the existence of unique featured CNFs not only has good adsorption ability for RhB molecules, but also benefits to the effective separation of photogenerated electron–hole pairs and thus improves the photocatalytic performance of the catalyst. Specially, the as-prepared Ag_3PO_4/CNFs/silica-fiber photocatalyst can easily reduce the cost for the practical application of Ag_3PO_4 photocatalyst. The new synthetic procedure is simple and could be applicable to a large number of efficient and inexpensive visible-light-driven photocatalytic materials.

1. Introduction

Recently, silver orthophosphate (Ag_3PO_4) has been regarded as a novel promising visible-light-driven photocatalyst for water splitting and organic contaminants elimination, owing to its superior photocatalytic properties compared with current photocatalysts [1–5]. However, Ag_3PO_4 photocorrosion easily occurs during a photocatalytic process when there are no electron acceptors present [6]. Furthermore, the utilization of nano-sized Ag_3PO_4 photocatalyst is considered to have higher efficiency, but it tends to lose activity rapidly [7]. It is also difficult for recovering the powered catalyst. Another two shortcomings are the slight solubility of Ag_3PO_4 in use and the relatively high cost of the starting material ($AgNO_3$) for its preparation and wide application [8]. These disadvantages preclude Ag_3PO_4 as a practical and applicable photocatalyst.

Studies have demonstrated that the synthesis of Ag_3PO_4 based photocatalyst with novel structure is one of the most promising and effective ways to overcome the above disadvantages of Ag_3PO_4 [9]. Note that loading and dispersing Ag_3PO_4 particles onto some suitable supports have been confirmed as effective ways to reduce Ag_3PO_4 content and to improve its photocatalytic efficiency and stability of Ag_3PO_4. Since the first publication on enhancing Ag_3PO_4 photocatalytic activity by using TiO_2 as support [8], Ag_3PO_4 composite photocatalysts such as Ag_3PO_4/carbon nanotubes [10], Ag_3PO_4/graphene [6,11], Ag_3PO_4/hydroxyapatite [12], Ag_3PO_4/sepiolite [13], Ag_3PO_4/bentonite [7,14], and Ag_3PO_4/$AlPO_4$-5 [15] have been reported to improve the performance of Ag_3PO_4 catalyst. Specially, the heterojunction system formation by loading and dispersion of Ag_3PO_4 particles onto some other semiconductor material is another optional way to accomplish the above-mentioned tasks. The reported semiconductor based supports include TiO_2 [8,16], $BiVO_4$ [17], CeO_2 [18], MoS_2 [19], WO_3 [20], Bi_2MoO_6 [21], $ZnFe_2O_4$ [22], BiOI [23], $BiPO_4$ [24], and so on. Although some special featured Ag_3PO_4 based materials (either by means of loading on some suitable support, or by means of heterojunction formation with other semiconductor material) have been reported to exhibit enhanced photocatalytic activities to some extents, taking an advantage over the corresponding powder Ag_3PO_4. It is still an urgent challenge to explore novel Ag_3PO_4 photocatalytic systems with low cost, good structure, high catalytic efficiency and stability.

In this paper, we firstly reported a successful and facile route for the fabrication of Ag_3PO_4/CNFs/silica-fiber hybrid composite via a combined chemical vapor deposition (CVD) technique and hydrothermal route. Note that the as-prepared Ag_3PO_4/CNFs/silica-fiber possessing a special novel structure was endowed with high photocatalytic efficiency toward the degradation of rhodamine B (RhB) under visible-light irradiation. More importantly, such facile

* Corresponding author. Tel.: +86 21 35303544; fax: +86 21 35303544.
E-mail address: qiangwu@shiep.edu.cn (Q. Wu).

http://dx.doi.org/10.1016/j.jtice.2016.03.029
1876-1070/

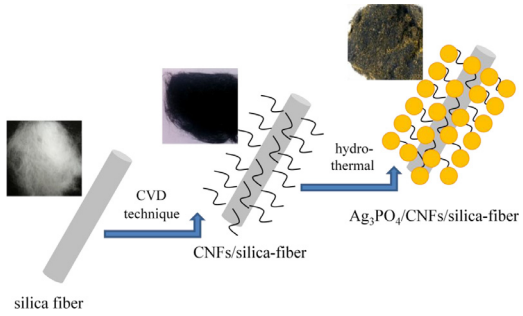

Scheme 1. Schematic illustration for the synthesis of Ag_3PO_4/CNFs/silica-fiber.

synthesis of Ag_3PO_4/CNFs/silica-fiber offers a good opportunity for low-cost, large-scale production of efficient visible-light-driven photocatalytic materials.

2. Experimental

2.1. Preparation of CNFs/silica-fiber

CNFs/silica-fiber was prepared by CVD technique (Scheme 1). Firstly, silica fiber (0.2 g) was immersed with 0.3 M $Ni(NO_3)_2$ acetone solution at room temperature. Afterwards, excess solution was removed by vacuum filtration and the resulting sample was further dried in air at 573 K for 1 h to get NiO/silica-fiber catalyst. Finally, decomposition of methane (flow rate = 320 mL min^{-1}) was performed over NiO/silica-fiber catalyst at 823 K for 2 h at atmospheric pressure to obtain CNFs/silica-fiber.

2.2. Synthesis of Ag_3PO_4/CNFs/silica-fiber composite

The synthesis of Ag_3PO_4/CNFs/silica-fiber was carried out using a hydrothermal route (Scheme 1): in a typical procedure, 2.04 g $AgNO_3$ and 0.57 g $Na_2HPO_4{\cdot}12H_2O$ was firstly dissolved in 20 mL deionized water under magnetic stirring for 30 min in different beaker, respectively. Afterwards, the obtained $AgNO_3$ aqueous solution was dropwise introduced into the obtained $Na_2HPO_4{\cdot}12H_2O$ aqueous solution. In the next step, CNFs/silica-fiber and a given amount of the above mixture precursor solution were both transferred into a 50 mL Teflon-lined autoclave for hydrothermal treatment at 473 K for 6 h. After reaction the autoclave was cooled to ambient temperature naturally. The obtained sample was finally washed with deionized water for three times and then dried at 383 K for 3 h to get the corresponding desired material. For comparison, solid Ag_3PO_4 powder was prepared by a hydrothermal process under the similar precursor concentration.

2.3. Characterization

X-ray diffraction (XRD) measurements were carried out on a BRUKER-D8 diffractometer with a Cu-Kα radiation. Field emission scanning electron microscopy (FE-SEM) measurements were performed by a Hitachi SU-1500 instrument. Ultraviolet–visible (UV–vis) diffuse reflectance spectroscopy was conducted on a Shimadzu UV-2550 spectrophotometer. Photoluminescence (PL) spectra were recorded on a Shimadzu RF-5301 spectrophotometer.

2.4. Evaluation of photocatalytic activity

The photocatalytic activity of the as-fabricated sample was evaluated by decomposition of RhB aqueous solution at room temperature in a home-made 100 mL glassy reactor. A 300 W Xe arc lamp (perfectlight co., PLS-SXE 300) equipped with an optical cutoff filter ($\lambda > 400$ nm) was used as a light source with 140 mW cm^{-2} illumination intensity. In a typical process, 0.10 g catalyst was dispersed in RhB solution (initial concentration C_0 is 20.0 mg L^{-1}). Before irradiation, the suspension was stirred in the dark for 35 min to establish an adsorption-desorption equilibrium between the photocatalyst and RhB. Then the solution was exposed to visible-light irradiation under magnetic stirring. The concentration of RhB (C_t) after a certain reaction time (t) was recorded. The degradation rate (D%) was calculated by equation: $D\% = (C_0 - C_t)/C_0 \times 100\%$, where C_0 and C_t represent the initial RhB concentration and RhB concentration after a certain reaction time (t), respectively. In addition, RhB photocatalytic degradation in the presence of Ag_3PO_4 powder was also performed for comparison.

3. Results and discussion

The phase structure of the as-prepared Ag_3PO_4/CNFs/silica-fiber sample was firstly examined by XRD pattern. For comparison, the XRD patterns of commercially available silica fiber and the synthesized CNFs/silica-fiber are also indicated in Fig. 1a and b. As expected, the XRD patterns of the Ag_3PO_4/CNFs/silica-fiber composite (Fig. 1c) match well with the polycrystalline structures of CNFs/silica-fiber and body-centered cubic Ag_3PO_4 (JCPDS No.06-0505), and rules out the possibility of any third phase formation. This means Ag_3PO_4/CNFs/silica-fiber hybrid composite was successfully prepared in the present study.

The morphology of the as-prepared Ag_3PO_4/CNFs/silica-fiber sample was further determined by FE-SEM and the representative image is shown in Fig. 2. As references, the morphologies of pure silica fiber and the synthesized CNFs/silica-fiber are also presented in Fig. 2. As shown in Fig. 2a, the typical morphology of silica fiber was straight with a relatively smooth surface, and its diameter was ca. 10 μm. Note that CVD process led to sample weight increase (from 0.2 g to 0.4 g) and a drastic color change (from white into black, Scheme 1). Fig. 2b and c shows the FE-SEM images of CNFs formed on silica fiber through CVD technique. It is obvious that large amounts of fibrous CNFs were entangled and uniformly formed on silica fiber. The average layer thickness of CNFs was calculated to be ca. 2.6 μm, and its diameters ranged from 50.0 to 80.0 nm. Fig. 2d and e illustrates the representative FE-SEM images of Ag_3PO_4/CNFs/silica-fiber via the combined CVD technique and hydrothermal process. As can be seen from Fig. 2d and e, agglomerative and irregular sphere-like Ag_3PO_4 particles with an average size of 100–200 nm was loaded on the surface of CNFs/silica-fiber. It should be pointed out that the total weight

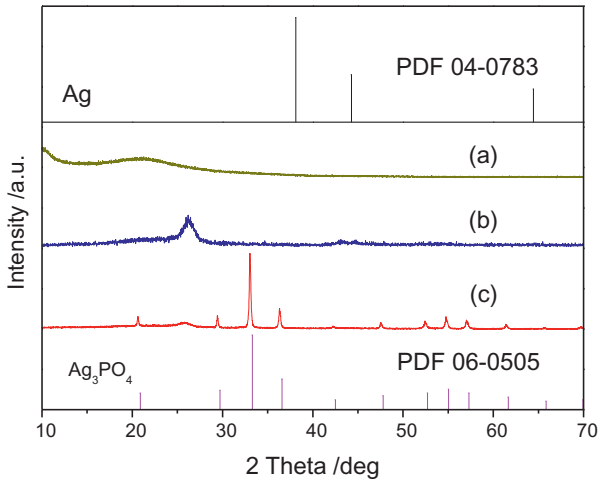

Fig. 1. XRD patterns of (a) silica fiber, (b) CNFs/silica-fiber, and (c) Ag_3PO_4/CNFs/silica-fiber.